

# Tunable pinning in superconducting films with magnetic microloops

A. V. Silhanek,<sup>a)</sup> W. Gillijns, and V. V. Moshchalkov

*Institute for Nanoscale Physics and Chemistry (INPAC), Nanoscale Superconductivity and Magnetism and Pulsed Fields Group, Katholieke Universiteit Leuven, Celestijnenlaan 200 D, B-3001 Leuven, Belgium*

V. Metlushko

*Department of Electrical and Computer Engineering, University of Illinois, Chicago, Illinois 60607*

B. Ilic

*Cornell Nanofabrication Facility, School of Applied and Engineering Physics, Cornell University, Ithaca, New York 14853*

(Received 15 August 2006; accepted 18 September 2006; published online 31 October 2006)

The authors study the flux pinning properties of superconductor/magnetic microring lattice hybrid structures. The used open triangular micromagnets represent an eightfold degree of freedom system, with six polarized and two flux-closure possible states. By conveniently choosing the magnetic state of the underlying rings, it is possible to induce different pinning potentials. They show that the magnetic vortex state with minimum stray field produces a weaker pinning in comparison with the polarized states. © 2006 American Institute of Physics. [DOI: 10.1063/1.2374798]

Regular arrays of nanoengineered pinning centers in conventional superconductors have proven to be an efficient way to enhance the critical current  $I_c$ . In general, the extent to which these centers influence the superconducting properties of the system depends on the details of the used nanostructuring. Nowadays it is possible to delineate a hierarchical list of different pinning sites going from the relatively weak blind holes,<sup>1</sup> in-plane and out-of-plane magnetic dots,<sup>2</sup> to the strong pinning produced by antidots.<sup>3</sup> For all these structures there is a natural limitation as they generate a nearly immutable pinning potential unable to be modified once defined.

Interestingly, as opposed to singly connected magnetic dots and nonmagnetic pinning structures, magnetic microloops can be readily set in several different magnetic states.<sup>4</sup> Each of these magnetic states interacts differently with the vortices in the superconductor, thus allowing one to control the easy direction of the vortex drift. It is particularly this remarkable flexibility to manipulate the vortex motion which makes this kind of pinning potentials attractive for practical applications although still a clear experimental corroboration is pending.

In this work we explore tunable pinning centers generated by an array of triangular rings and demonstrate that by changing the magnetic state of the underlying microloops it is possible to modify the pinning properties of the superconductor. In particular, we show that the flux-closure magnetic vortex state represents a less efficient pinning potential compared with the polarized state.

The used sample consists of a closely packed square array of cobalt equilateral triangular loops (250 nm wide, 23 nm thick, with lateral size  $d=2\ \mu\text{m}$  and separated by  $s=250\ \text{nm}$  from the neighboring elements) fabricated by electron-beam lithography and lift-off on a silicon wafer. A scanning electron microscope (SEM) image of the array is shown in Fig. 1(a). We evaporated a 5 nm thick Ge layer on top to avoid proximity effects<sup>5</sup> and then a superconducting Pb film (thickness  $t=25\ \text{nm}$ , critical temperature  $T_c$

$=7.220\ \text{K}$ , residual resistivity ratio of  $\sim 15$ , and electronic mean free path<sup>6</sup>  $\ell \sim 80\ \text{nm}$ ) which is covered with a protective 20 nm thick Ge capping layer. In order to ensure a homogeneous current distribution, the continuous Ge/Pb/Ge trilayer is patterned into a transport bridge by optical lithography and ion-mill etching. The  $400\ \mu\text{m}$  wide transport bridge is aligned along the  $-x$  direction as schematically indicated in Fig. 1(a). In this way the Lorentz force lies along the higher symmetry axis of the underlying array. The vortex pinning properties of this hybrid sample were investigated by electrical transport measurements using a Quantum Design cryostat with conventional electronics.

It is worth noticing that if solid singly connected triangles are used as in Ref. 7, a flux-closure state with a strong  $z$  component in the middle of the triangle is formed.<sup>4</sup> In contrast to this, ring structures favor a flux-closure state because the highly energetic vortex core is removed.<sup>8</sup> Inserts (b) and (c) in Fig. 1 show two typical magnetic states of

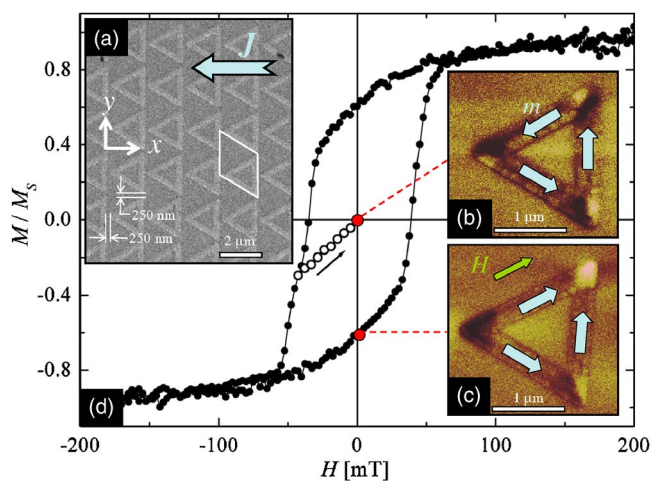


FIG. 1. (Color online) (a) SEM image indicating the used spatial coordinates and the unit cell of the pinning array, (b) magnetic vortex, and (c) polarized states as seen by MFM. (d) Magnetic hysteresis loop  $M(H)$  of the Co ring array at  $T=10\ \text{K}$  for  $\mathbf{H} \parallel \mathbf{y}$  normalized to its saturation value  $M_s = 911\ \text{emu/cm}^3$ . Open symbols correspond to the flux-closure state.

<sup>a)</sup>Electronic mail: alejandro.silhanek@fys.kuleuven.be

triangular ring elements measured by magnetic force microscopy (MFM). If a magnetic field  $H$  higher than the saturation value is applied along one of the sides of the triangle, the element is magnetized into a single domain state with in-plane magnetization. A full magnetization loop  $M(H)$  at  $T = 10$  K for applied field  $\mathbf{H}$  along the  $\mathbf{y}$  direction as determined by superconducting quantum interference device measurements is shown in Fig. 1(d).<sup>9</sup>

When a large magnetic field higher than saturation field is applied parallel to the edge direction, the ring is magnetized into a single domain state. The domain walls are formed as the magnetic field is reduced to zero. The exact magnetic patterns depend on the magnetic history. When  $H$  is reversed to about  $-43$  mT and then reduced to zero [open symbols in Fig. 1(d)], domain walls are formed as shown in Fig. 1(b). At the three different corners the magnetic moment gradually rotates by  $120^\circ$ .<sup>10</sup> However, if starting from the single domain fully polarized state  $H$  is directly reduced to zero, a different domain pattern is observed [see Fig. 1(c)]. Now at the lower right corner of the ring, the magnetic moment gradually rotates by  $120^\circ$ , whereas at the other two corners the magnetic moment form either transverse- or vortex-type domain walls. In this case the stray field contrast of the  $z$  component, indicated in the inserts as white and black spots, is much stronger than for the  $120^\circ$  walls. Object oriented micromagnetic simulations suggest that each of the three segments of the triangular shaped rings are nearly single domain states, as indicated by the arrows in Figs. 1(b) and 1(c). Different orientations of these single domain states form different domain patterns. As a result the triangular shaped rings have two vortex states of opposite chirality and six polarized states. The type and orientation of the elements can be controlled by a small external in-plane magnetic field. For detailed description of magnetization process in triangular ring, we refer the readers to Refs. 10 and 11.

It has been previously shown that for pinning purposes, only the out-of-plane component of the stray field counts.<sup>12</sup> This effect suggests that in our case the pinning efficiency can be tuned from weak to strong limits by simply switching from flux-closure to the polarized magnetic state of the Co loops. In order to check whether the magnetic state of the underlying micromagnets indeed influences the superconducting properties of the thin film, we first determined the normal-superconductor (N/SC) phase boundary. Figure 2(a) shows the N/SC transition as estimated by 10% of the normal state resistance  $R_n$  for two of the magnetic states and compares it with the results for a simultaneously grown plain film. The plain film exhibits a featureless nearly linear upper critical field  $H_{c2}(T)$  from which it is possible to estimate a superconducting coherence length  $\xi(0) = 33 \pm 3$  nm. In the case of the Pb film with the array of triangles underneath, a parabolic background is observed around  $H=0$  regardless of the initial magnetic state. A similar behavior has been reported for ferromagnet/superconductor bilayers<sup>13</sup> and samples with square arrays of holes.<sup>14</sup> In our sample this transition from linear to parabolic field dependence occurs at  $T_o \approx 7.16$  K where  $1.8\xi(T_o) \sim 1.26 \mu\text{m}$  exceeds the size  $w$  of the domains where superconductivity first nucleates.<sup>14</sup> For higher temperatures the phase boundary can be approximated by<sup>15</sup>  $T_c(H)/T_c(0) = 1 - (\alpha H)^2$ , with  $\alpha = \xi(0)\pi w/2\sqrt{3}\phi_0$  and  $\phi_0$  the flux quantum. Using this expression to fit the data in Fig. 2(a), we obtain  $w \sim 1.26 \mu\text{m}$  which agrees with the estimation obtained above from the coherence length.

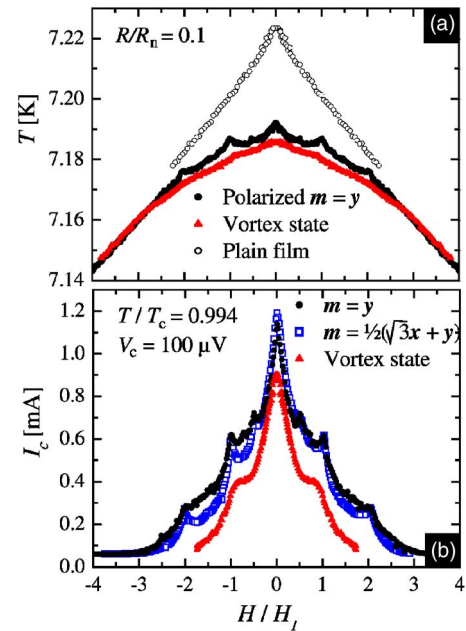


FIG. 2. (Color online) (a) N/SC phase boundary estimated by 10%  $R_n$  criterion for a reference plain film and a film on top of Co ring array in the flux-closure and polarized states. (b) Critical current estimated by  $100 \mu\text{V}$  criterion at  $T/T_c = 0.994$  for the magnetic closure state and the  $\mathbf{m} = \mathbf{y}$  and  $\mathbf{m} = \frac{1}{2}(\sqrt{3}\mathbf{x} + \mathbf{y})$  polarized states.

From Fig. 2(a) it is apparent that the patterned sample exhibits clear commensurability features at  $nH_1$ , with  $n = \frac{1}{2}, 1, \frac{3}{2}, 2$  and  $H_1 = \phi_0 / ((d \cos(\pi/6) + s)(d + s)) = 0.465$  mT [the unit cell is shown schematically in Fig. 1(a)]. Furthermore, a direct comparison of the phase boundary for the magnetic vortex state with the magnetized state indicates that matching features, and therefore collective effects, are far less prominent in the flux-closure vortex state. This effect is a direct consequence of the different stray fields generated by these two magnetic states.

Although the flux line lattice configuration at the main matching fields is expected to follow the rectangular symmetry of the underlying magnetic landscape,<sup>16</sup> it is not trivial to determine where actually the vortices locate within the unit cell. In the magnetized state two different scenarios may arise as to whether the stray field associated with the in-plane dipole can generate a vortex-antivortex pair or not. If there is no vortex-antivortex pair, then flux lines sit on top of the positive  $z$  component of the stray field; otherwise flux lines will be attracted by the antivortices generated by the stray field and thus sit close to the maximum negative  $z$  component.

In the magnetic vortex state, the three identical domain walls at the vertices of the triangles do not impose any preferential pinning for an isolated element. However, if  $\xi(T) > s$  this threefold degeneracy is lifted by the close proximity between two adjacent triangles and vortices sit where the stray field maximizes. This is consistent with the fact that matching features in all cases are visible only for  $T > 7.16$  K where  $\xi(T) > 0.45 \mu\text{m} > s$ .

Let us now focus on the flux pinning properties of the system. To that end we measured the critical current  $I_c(H)$  at  $T/T_c = 0.994$  using a voltage criterion of  $100 \mu\text{V}$  for three contrasting magnetic states as shown in Fig. 2(b). The  $\mathbf{m} = \frac{1}{2}(\sqrt{3}\mathbf{x} + \mathbf{y})$  magnetized state is built by applying an in-plane field  $150^\circ$  off the current direction, whereas for the  $\mathbf{m} = \mathbf{y}$

state the in-plane field is applied perpendicular to the current direction. In the  $\mathbf{m}=\mathbf{y}$  state the pinning force is maximum and therefore an optimal pinning efficiency is expected in agreement with the observed behavior. At the commensurability fields, the vortex lattice is very stable (elastic constants have a local maximum) and the difference between the two magnetic states becomes negligible. The most striking behavior, however, appears when the magnetic triangles are set in the vortex state. Here, the critical current is substantially *reduced* and only commensurability at  $H_1$  *remains*. A similar result has been reported by Van Look *et al.*<sup>12</sup> for an array of magnetic dots although in that work a much more complicated demagnetization protocol was followed. The lack of features at rational matching fields in the flux-closure state can be ascribed to the weaker pinning potential which favors a more disordered flux line lattice. At lower temperatures (not shown) a kink in  $I_c(H)$  at  $H=2H_1$  is still visible although less pronounced than for the polarized magnetic rings.

To summarize, we have explored the dynamic pinning properties of a conventional superconductor on top of an array of micromagnets composed by Co open triangles. We show that the system studied represents a very flexible and controllable flux pinning structure. The used triangular shape of the magnets gave us full control of the chirality of the flux-closure state and the possibility to induce six different dipolar states by following very simple magnetization protocols. A clear contrast in the vortex pinning properties of the flux-closure and the polarized states is observed.

One of the authors (V.M.) acknowledge funding support from U.S. NSF, Grant Nos. ECS-0202780 and DMR-

0210519. Another author (A.V.S.) is grateful for the support from the FWO-Vlaanderen. This work was also partially supported by the GOA project.

<sup>1</sup>S. Raedts, A. V. Silhanek, M. J. Van Bael, and V. V. Moshchalkov, Phys. Rev. B **70**, 024509 (2004).

<sup>2</sup>I. F. Lyuksyutov and V. L. Pokrovsky, Adv. Phys. **54**, 67 (2005).

<sup>3</sup>M. Baert, V. V. Metlushko, R. Jonckheere, V. V. Moshchalkov, and Y. Bruynseraede, Phys. Rev. Lett. **74**, 3269 (1995).

<sup>4</sup>R. P. Cowburn, J. Phys. D **33**, R1 (2000); D. K. Koltsov, R. P. Cowburn, and M. E. Welland, J. Appl. Phys. **88**, 5315 (2000).

<sup>5</sup>A. I. Buzdin, Rev. Mod. Phys. **77**, 935 (2005).

<sup>6</sup>This value was estimated using  $\rho_n \ell = 1 \times 10^{-5} \mu\Omega \text{ cm}^2$  [J. J. Hauser, Phys. Rev. B **10**, 2792 (1974)] where  $\rho_n$  is the normal state resistivity at  $T = T_c$ .

<sup>7</sup>J. E. Villegas, S. Savel'ev, F. Nori, E. M. Gonzalez, J. V. Anguita, R. Garcia, and J. L. Vicent, Science **302**, 1188 (2003).

<sup>8</sup>We have found experimentally that for separations between adjacent triangles larger than 100 nm, no magnetic interaction is expected and thus each triangle can be regarded as an isolated element.

<sup>9</sup>Almost no temperature dependence of the magnetization was observed for  $10 \text{ K} < T < 300 \text{ K}$ .

<sup>10</sup>A. Imre, L. Ji, A. Orlov, G. Bernstein, W. Porod, E. Varga, B. Ilic, and V. V. Metlushko, IEEE Trans. Magn. (to be published).

<sup>11</sup>P. Vavassori, O. Donzell, M. Grimsditch, V. Metlushko, and B. Ilic, J. Appl. Phys. (unpublished).

<sup>12</sup>L. Van Look, M. J. Van Bael, K. Temst, J. G. Rodrigo, M. Morelle, V. V. Moshchalkov, and Y. Bruynseraede, Physica C **332**, 356 (2000).

<sup>13</sup>M. Lange, M. J. Van Bael, and V. V. Moshchalkov, Phys. Rev. B **68**, 174522 (2003).

<sup>14</sup>E. Rosseel, T. Puig, M. Baert, M. J. Van Bael, V. V. Moshchalkov, and Y. Bruynseraede, Physica C **282-287**, 1567 (1997).

<sup>15</sup>V. V. Moshchalkov, V. Bruyndoncx, E. Rosseel, L. Van Look, M. Baert, M. J. Van Bael, T. Puig, C. Strunk, and Y. Bruynseraede, AIP Conf. Proc. **427**, 171 (1998).

<sup>16</sup>O. M. Stoll, M. I. Montero, J. Guimpel, J. J. Akerman, and I. K. Schuller, Phys. Rev. B **65**, 104518 (2002).